Eur. Phys. J. B **49**, 135–140 (2006)
DOI: 10.1140/epjb/e2006-00043-y

THE EUROPEAN PHYSICAL JOURNAL B

Lower critical field and intragrain critical current density in the ruthenate-cuprate $RuSr_2Gd_{1.5}Ce_{0.5}Cu_2O_{10}$

M.G. das Virgens[1,2], S. Garcia[1,3,a], and L. Ghivelder[1]

[1] Instituto de Física, Universidade Federal do Rio de Janeiro, C.P. 68528, Rio de Janeiro, RJ 21941-972, Brazil
[2] Instituto de Física, Universidade Federal Fluminense, Niterói, RJ 24210-340, Brazil
[3] Laboratorio de Superconductividad, Facultad de Física-IMRE, Universidad de La Habana, San Lázaro y L, Ciudad de La Habana 10400, Cuba

Received 19 August 2005 / Received in final form 16 November 2005
Published online 17 February 2006 –

Abstract. The lower critical field of the grains, H_{c1}, and the intragrain critical current density, J_c, were determined for the superconducting ruthenate-cuprate $RuSr_2Gd_{1.5}Ce_{0.5}Cu_2O_{10-\delta}$ [Ru-1222(Gd)] through a systematic study of the hysteresis in magnetoresistance loops. A reliable method, based on the effects of the magnetization of the grains on the net local field at the intergranular junctions is provided, circumventing the problem of the strong masking of the superconducting diamagnetic signal by the ferromagnetic background. The temperature dependency of H_{c1} and J_c both exhibit a smooth increase on cooling without saturation down to $T/T_{SC} \cong 0.2$. The obtained H_{c1} values vary between 150 and 1500 Oe in the $0.2 \leq T/T_{SC} \leq 0.4$ interval, for samples annealed in an oxygen flow; oxygenation under high pressure (50 atm) leads to a further increase. These values are much larger than the previously reported rough assessments (25–50 Oe), using conventional magnetization measurements. High J_c values of $\sim 10^7$ A/cm^2, comparable to the high-T_c cuprates, were obtained. The $H_{c1}(T)$ and $J_c(T)$ dependencies are explained in the context of a magnetic phase separation scenario.

PACS. 74.72.-h Cuprate superconductors (high-T_c and insulating parent compounds) – 74.25.Fy Transport properties (electric and thermal conductivity, thermoelectric effects, etc.) – 74.25.Ha Magnetic properties

1 Introduction

Since the discovery of the so called magnetic superconductors $RuSr_2RCu_2O_8$ (Ru-1212) and $RuSr_2(R,Ce)_2Cu_2O_{10-\delta}$ (Ru-1222), with R = Gd, Eu [1,2], considerable effort has been devoted to the understanding of the interplay between the ferromagnetic (FM) component, emerging from the long-range order of the Ru moments, and the onset of the superconducting (SC) state [3]. Among several important topics, the possibility of π-phase formation across the RuO_2 layers [4–6], the itinerant or localized character of the magnetism of the Ru moments [7–9], the magnetic phase separation scenario of nanoscale FM clusters with superconductivity nucleating only in the surrounding antiferromagnetic matrix [10,11], and the possibility of triplet paring [8], have been considered to explain how this puzzling coexistence may occur. On the other hand, some important superconducting parameters have been less thoroughly investigated. Reports include the determination of the coherence length ξ and the higher critical field H_{c2} [12–14], and the intragrain London penetration length λ_L [11,15–17], and rough estimations of the lower critical field of the grains, H_{c1} [18]. In relation to the determination of H_{c1}, a diamagnetic signal has been observed in a few cases at the low field range of the $M(H)$ magnetization loops in Ru-1222, with a negative minimum at about 25 Oe [18] and 50 Oe [19,20].

There are also fewer studies on relevant intrinsic superconducting properties, such as the intragrain critical current density, J_c [21], mainly because the strong FM contribution to the magnetization from the Ru sublattice makes impracticable the use of the magnetic hysteresis loops to determine both H_{c1} and J_c. In the present study we overcome this intrinsic difficulty and present a reliable method to determine these magnitudes and their temperature dependencies in Ru-1222(Gd), through a systematic study of the hysteresis in the isotemperature magnetoresistance $R(H)$ curves. Since no single crystals are available for this compound, polycrystalline materials were used in the present investigation. Two different Ru-1222(Gd) samples were studied, obtained under different partial

[a] e-mail: sgg@if.ufrj.br

oxygen pressures. At variance with the behavior of the high-T_c cuprates, a monotonic increase without saturation in both H_{c1} and J_c on cooling was observed, reaching values as high as $H_{c1} \sim 1000$ Oe and $J_c \sim 10^7$ A/cm^2, at $T = 7.5$ K. A comparison with $YBa_2Cu_3O_7$ (YBCO) and with the results reported for modeling the magnetic properties of Ru-1212 on the basis of the theory of the SC/FM multilayers is presented.

2 Experimental

Polycrystalline $RuSr_2Gd_{1.5}Ce_{0.5}Cu_2O_{10-\delta}$ was prepared by conventional solid-state reaction using an oxygen flow in the final heat treatment. The room temperature X-ray diffraction pattern corresponds to Ru-1222(Gd), with no spurious lines. Scanning electron microscopy revealed a dense grain packing, with an average grain size d $\cong$ 0.5−1 μm. More details on sample preparation and microstructure can be found elsewhere [22]. After characterization, the as-prepared (*asp*) sample was annealed for 24 h at 600 °C under 50 atm of pure oxygen [high oxygen pressure (*hop*) sample]. Magnetotransport and ac magnetic susceptibility measurements [22] reproduce the behavior of good quality samples [8]. Bars of $\cong$10 mm in length and 0.6 mm^2 cross sectional area were cut from the sintered pellet. The resistance was measured with a standard four contacts probe using a Quantum Design PPMS system, at $T = 7.5$, 8, 9, 10, 11.25, 12.5, and 15 K for the *asp* sample; the *hop* sample was also measured at 8.5 K. A large number of $R(H)$ curves were collected for each temperature to accurately follow the different characteristic regimes found in the magnetoresistance response (as described below), and to warrant a reliable quantitative determination of the fields at which the transition from one regime to another occur. The most relevant experimental parameter varied experimentally is the maximum applied field within the $R(H)$ curves, H_{max}, which ranged from a few tens of Oe up to 60 kOe.

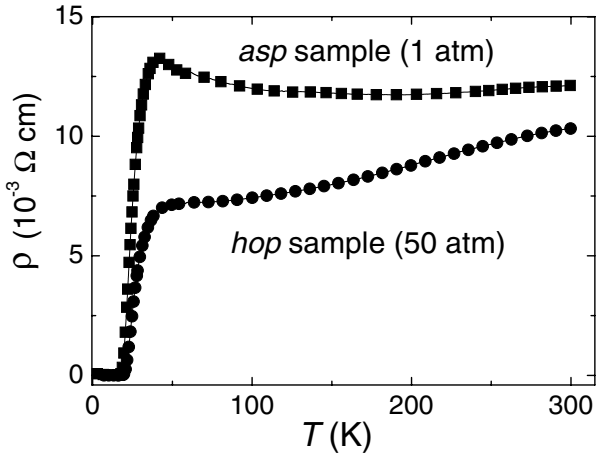

Fig. 1. Temperature dependence of the resistivity for the Ru-1222 samples obtained under oxygen pressure of 1 atm (*asp* sample) and under high oxygen pressure of 50 atm (*hop* sample).

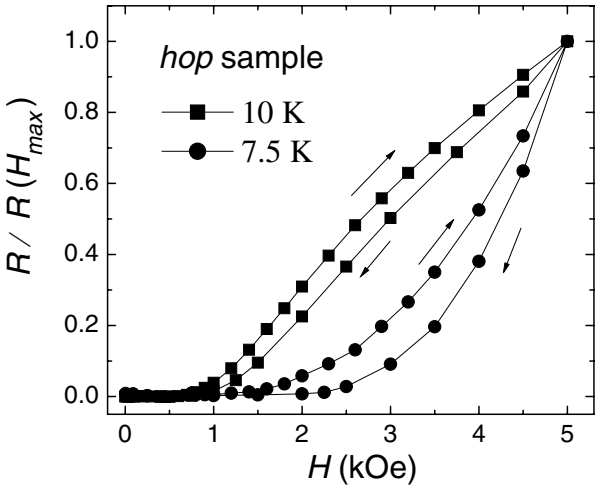

Fig. 2. Selected isothermal hysteresis loops of the magnetoresistance of Ru-1222 *hop* sample, measured with $H_{max} = 5$ kOe at $T = 7.5$ and 10 K. The arrows indicate the field direction during the measurement. The curves are normalized to the maximum resistance value, $R(H_{max})$.

3 Results

In order to characterize the transport behavior of the studied samples we initially measured the temperature dependence of the resistivity. It is clear from the data shown in Figure 1 that oxygenation under pressure strongly reduces the absolute resistivity values, enlarges the linear behavior of the normal-state region, and reduces the width of the SC transition. In addition, the superconducting transition temperature, $T_{SC} \cong 45$ K, as determined from the peaks in the derivative of the resistivity for the as prepared (*asp*) sample, increases by approximately 3 K in the *hop* sample. These features agree with previous reports in good quality materials [7,8]. The present study concentrates in results of resistance as a function of field, $R(H)$, measured at fixed temperature with different maximum fields, H_{max}, in each sweep. Four different behaviors were identified in the $R(H)$ curves as H_{max} is increased: a) a zero resistance region, typically for $H_{R=0} < 100$ Oe; b) an interval of reversible dissipation up to an irreversible field H_{irr}, from about 150 Oe to 1500 Oe for the *asp* sample and up to 3000 Oe for the *hop* sample; c) an H_{max}-dependent hysteretic behavior, and d) an hysteretic response independent of H_{max}. Figure 2 shows selected magnetoresistance hysteresis loops for the *hop* sample with $H_{max} = 5000$ Oe, measured at $T = 7.5$ and 10 K, normalized to the $R(H_{max})$ values. For each temperature, loops similar in shape but broader were obtained for the *asp* sample. In the hysteretic region the resistance curves measured with decreasing external field, $R(H \downarrow)$, are always below the corresponding virgin curves, $R(H \uparrow)$, measured with increasing field. When the difference $\Delta R(H) = R(H \uparrow) - R(H \downarrow)$ is plotted, a peak is always obtained at a certain intermediary value of the applied field, H_{ext}. With the rise in H_{max}, the peak gradually

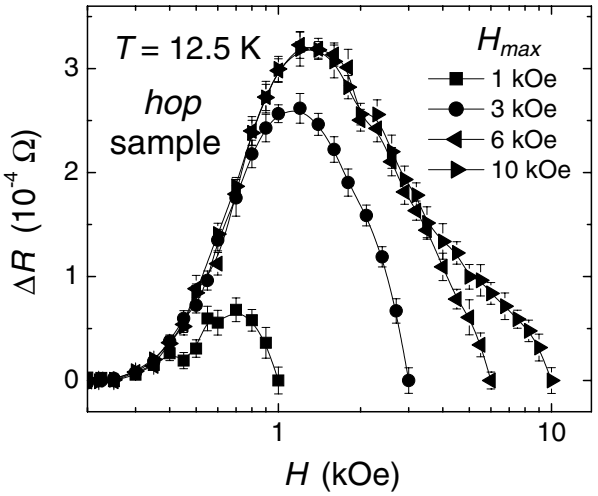

Fig. 3. Field dependence of the difference between the virgin and the decreasing field magnetoresistance curves, $\Delta R(H) = R(H\uparrow) - R(H\downarrow)$, measured at $T = 12.5$ K for Ru-1222 *hop* sample with different H_{max}. The peak shifts to higher fields and increases its amplitude with the rise in H_{max} up to a certain saturation field H_{sat}.

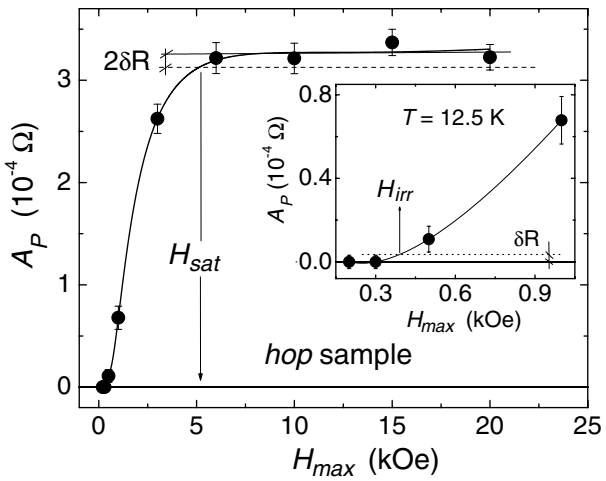

Fig. 4. Amplitude A_P of the peak in $\Delta R(H) = R(H\uparrow) - R(H\downarrow)$, plotted as a function of the maximum applied field H_{max} for Ru-1222 *hop* sample at T= 12.5 K. The continuous line is a polynomial fitting. The straight line is a fit of the experimental points in the plateau observed in the high H_{max} range. The dashed line shows the error in the determination of A_P, measured from the plateau level. The saturation field H_{sat} is indicated. The inset shows an enlarged section of the low H_{max} region. The dotted line marks the error level in the determination of the magnetoresistance. The irreversible field H_{irr} is indicated.

increases its amplitude, $A_P(H_{max})$, and shifts to higher H_{ext} values until a certain field $H_{max} \equiv H_{sat}$ is reached, that we denote as a saturation field. For H_{max}>H_{sat} the peak in $\Delta R(H)$ remains unchanged. To illustrate this behavior, Figure 3 plots $\Delta R(H)$ as a function of H_{ext} for different values of H_{max}, for the *hop* sample at $T = 12.5$ K.

We focus our attention on a careful determination of H_{irr} and H_{sat}. Since $R(H\downarrow)$ diverge smoothly from $R(H\uparrow)$, it is necessary to implement a method for this evaluation. We proceeded as follows: a) the error $\delta R(H)$ in the determination of $R(H)$ was taken as the average of the standard deviations of each measured experimental point in a given loop; we found that successive $R(H)$ curves measured at each temperature for different H_{max} (typically 15–20 curves) always fell inside this $\delta R(H)$ criterion; b) for each temperature, A_P was plotted as a function of H_{max}, as shown in Figure 4 for the *hop* sample at $T = 12.5$ K, and the data fitted using a polynomial function; the error in the determination of A_P is $2\delta R(H)$; c) $R(H\downarrow)$ is considered reversible if $A_P(H_{max})$ does not exceed the $\delta R(H)$ threshold, as indicated by a dotted line above the zero resistance level in the inset of Figure 4 (low H_{max} region); the irreversibility field, H_{irr}, is determined from the intersection of the fitted polynomial function with the $\delta R(H)$ level (Fig. 4, inset); d) the plateau observed for $A_P(H_{max})$ for the high H_{max} range was fitted by a straight line parallel to the H_{max} axis (continuous line in Fig. 4, main panel); e) the saturation field, H_{sat}, was determined as the field for which the polynomial function diverges in $2\delta R(H)$ from the fitted straight line, (intersection with the dashed line, parallel and below the plateau level in Fig. 4, main panel). As we discuss below, H_{irr} is a good estimation of the lower critical field of the grains, H_{c1}.

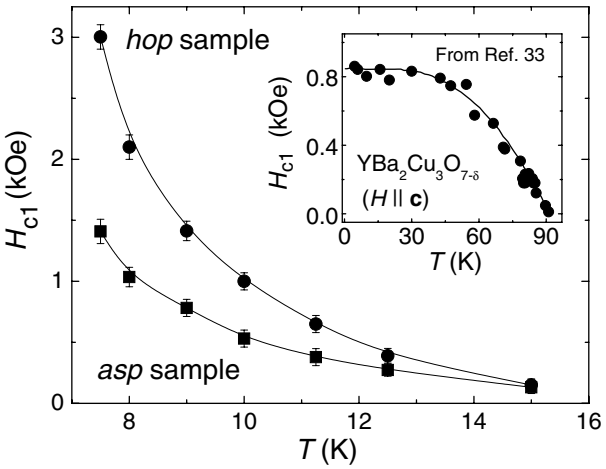

Fig. 5. Temperature dependence of the lower critical field of the grains H_{c1} for both Ru-1222 *asp* and *hop* samples. The behavior of H_{c1} (parallel to the c axis) for $YBa_2Cu_3O_7$, obtained from reference [33] is also shown for comparison. The continuous lines are guides to the eyes.

The temperature dependencies of H_{c1} and H_{sat} for the *asp* and *hop* samples are plotted, in Figure 5 and in the inset of Figure 6, respectively. The behavior of H_{c1} for YBCO (with the field parallel to the sample's c axis) is also shown for comparison in the inset of Figure 5. The $H_{c1}(T)$ and $H_{sat}(T)$ curves for both samples monotonically decrease with the increase in temperature and smoothly merge at about 15 K. The values of J_c at different temperatures, determined by using the Bean critical

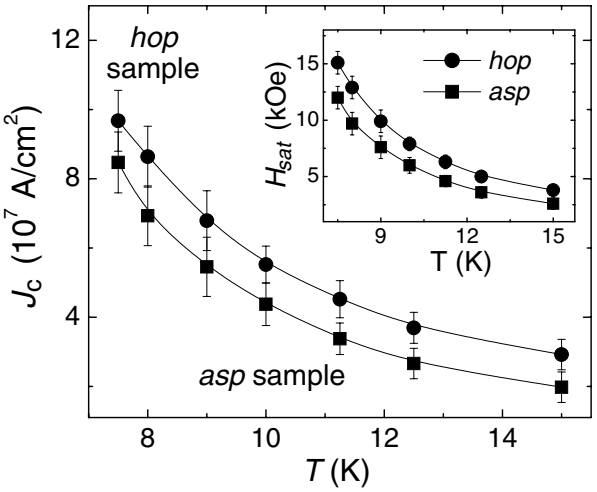

Fig. 6. Temperature dependence of the intragrain critical current density J_c for both Ru-1222 *asp* and *hop* samples. The inset shows the temperature dependence of the saturation field H_{sat}. The continuous lines are guides to the eyes.

state model [23], as described below, are shown in Figure 6. A systematic increase of J_c on cooling is found, with slightly higher values for the *hop* sample.

4 Discussion

A key point to understand the features of the $R(H)$ curves is to recognize that the magnetization in the grains contributes to the effective local field at the intergranular junctions. Hysteresis in the magnetoresistance was recently observed in ceramic Ru-1222 samples [24], and a preliminary analysis evidenced that the granular character of the material is relevant. Unlike Ru-1212, in Ru-1222 the coercive field and the remanent magnetization vanish at the SC transition, $T_{SC} \cong 45\ K$, for both Gd [18,25] and Eu [20,26,27] based compounds, even though the magnetic transition temperatures are much higher. Since the Gd ions are decoupled from the Ru moments [28,19,29], no changes in the irreversibility behavior are observed when Gd is replaced in Ru-1222 by Eu. The essential structure governing the irreversibility response in Ru-1222 is the thick $(R,Ce)_2O_2$-fluorite-type blocks separating the RuO_2 planes. The large separation distance strongly weakens the superexchange interactions between the magnetic layers, which are weakly coupled through dipole-dipole interaction [30,22]. Therefore, the hysteretic behavior of the $R(H)$ curves has a SC origin in Ru-1222.

For a low applied magnetic field, H_{ext}, the net local field at the intergranular junctions is not strong enough to destroy all the SC percolative paths across the weak-linked network, leading to the observed zero resistance region in $R(H)$. For $H_{ext} > H_{R=0}$, the connectivity of the network is affected in such extent that the current across the sample can not flow without dissipation, and a sizable resistance appears. The existence of a reversible dissipation section in the $R(H)$ curves evidence that the grains have not yet been penetrated at this field range, and there is no intergranular pinning. Irreversible $R(H)$ loops appear when the local field at the junctions penetrates the grains. For polycrystalline high-T_c cuprates this local field is higher than H_{ext} due to flux compression associated to diamagnetic shielding, leading to an underestimation of H_{c1}. For Ru-1222, the contribution of the FM magnetization to the local field at the intergranular network, H_{Ru}, is oriented in opposition to H_{ext}, diminishing the flux compression effect. It was recently determined that H_{Ru} is approximately 15 Oe at $T = 0$ K for Ru-1222 [31]. Since H_{irr} varies from 100 to 3000 Oe, any possible difference between the local penetration field of the grains and H_{ext} due to the contribution of H_{Ru} is approximately 10% or less. Therefore, by determining H_{irr} one obtain a good estimation of H_{c1}.

Let us consider the effects of the flux trapped in the grains on the $R(H)$ loops. For a given $H_{max} > H_{c1}$, a fraction of the grain volume is penetrated. When H_{ext} is decreased different field profiles are created inside the grains due to pinning, gradually evolving as H_{ext} diminishes [23]. Each field profile represents a spatial circulation of currents, i.e., a certain SC magnetization, contributing with a local field H_{SC} at the intergranular junctions. The lowest value of H_{ext} at which full reversal is obtained is $H_{ext} = H_{c1} + 2H^*$ [32].Until the fully reversed profile is not attained, the exact value of H_{SC} for a given H_{ext} in the returning curve changes as H_{max} increases, because a different field profile is obtained for that external field.

The extent of the compensation between H_{ext} and H_{SC} at the junctions as the returning curves are collected is clearly evidenced by the changes in the maxima of $A_P(H_{max})$, the amplitude of the peak in $\Delta R(H)$, as shown in Figure 3. The peaks correspond to a maximum average compensation of the local fields in the polycrystal, a relative maximum in the connectivity of the weak-linked network, as H_{ext} is decreased. The increase in amplitude of the peaks for higher H_{max} is associated to a narrowing of the distribution of local fields in the sample as the SC magnetization of the grains rises. The position of the peaks is shifted to higher fields with the rise in H_{max} up to H_{sat}, because the field profile inside the grains becomes reversed in a larger extent, gradually leading to a higher H_{SC} in opposition to H_{ext}; the maximum compensation occurs at higher H_{ext}. Once the external field is high enough to reach the fully reversed profile there will be no further increase in H_{SC} with the rise in H_{max}, and the $A_P(H_{max})$ maxima remain unchanged. Therefore $H_{sat} = H_{c1} + 2H^*$. Since the FM contribution to the local field is not hysteretic, it has no effect on H_{sat}.

Let us compare the absolute values and temperature dependence of H_{c1} in Ru-1222 with YBCO. Due to the wide SC transition width in the former, the higher temperature for which H_{c1} was determined is $T = 15$ K ($T/T_{SC} \cong 0.3$). For this T/T_{SC} value, the lower critical field in YBCO has already reached its saturation value, $H_{c1}(\text{YBCO}) \cong 850$ Oe [33] (with H parallel to the c-axis), while it is only 150 Oe for both Ru-1222 samples. However, due to its monotonic increase on cooling, H_{c1} reaches

a value twice larger than YBCO for the Ru-1222 *asp* sample, and even higher for the *hop* one (3000 Oe) at 7.5 K ($T/T_{SC} \cong 0.2$).

At this point it is important to consider whether there is a possible contribution from surface barriers in the determination of H_{c1}. It should be noted that Ru-1222 exhibits a monotonic increase of $1/\lambda^2(T)$ on cooling without saturation down to $T = 5$ K [11], at variance with the high-T_c cuprates. This implies a reduced efficiency of any possible barrier shielding with the decrease in temperature, since a decrease in λ favours the flux penetration through weak spots at the grain surface. Another important point is the strong decrease in $\lambda(T)$ in samples with higher partial oxygen pressure during the final heat treatment [11]. Therefore, flux penetration through the weak spots must be easier for the *hop* sample in comparison to the *asp* one, and the higher H_{c1} values obtained for the former can not be explained as due to surface barriers. In addition, Ru-1212 and Ru-1222 present a very distinctive structural feature: the existence of sharp antiphase boundaries with local distortions separating structural domains of coherently rotated RuO_6 octahedra. A high density of quite sharp boundaries, of several tens of unit cells in length, have been observed in high resolution transmission electron microscopy images [34]. In ceramic superconductors, long-range distortions, as twinning planes [35] and columnar defects [36], are known to act as channels for flux penetration, dramatically suppressing surface barriers shielding. Antiphase boundaries should work very similarly. These considerations strongly indicate that surface barriers effects are not the source of the observed H_{c1} dependence in polycrystalline Ru-1222.

The large H_{c1} values obtained at low temperatures are somewhat unexpected since, as mentioned above, previous reports based on $M(H)$ curves inferred H_{c1} values as low as 25–50 Oe in Ru-1222 [18–20]. Nevertheless, clear evidence that these reports greatly underestimate the magnitude of H_{c1} comes from measurements in samples with partial substitution of Ru by non-magnetic elements. The negative diamagnetic minimum in $M(H)$ is shifted to ∼300 Oe for 30% substitution of Ru by Sn [37], and 40% substitution by Nb [38], even though T_{SC} is decreased in both cases. Moreover, the zero net magnetization point in the virgin $M(H)$ curves (for which a significant diamagnetic signal is still present) is observed for $H_{ext} \sim 800$ Oe in both systems. These results indicate that the masking effect of the FM background is strong, and that the actual magnitude of H_{c1} is in fact considerably higher. Further evidence of H_{c1} values of the order of several hundreds Oe in ruthenate-cuprates comes from the magnitude of the internal Ru magnetization and the local fields at different points of the cell. It has been determined that the in-plane magnetization at the RuO_2 layers is $4\pi M \sim 4$ kG, yielding a macroscopic (cell volume average) dipolar internal field $B_{int} = 4\pi\langle M\rangle = 700$ Oe [4]. The latter value is confirmed by Gd^{3+}-electron spin resonance [39] and muon spin rotation [40] measurements, giving internal fields of ∼600–700 Oe at the Gd site and near to the apical oxygen of the CuO_5 pyramid, respectively. Flux expulsion from the grains can occur only if, at a certain sufficiently low temperature, $H_{c1}(T)$ exceeds the magnetization value of $4\pi M$. This "internal" Meissner effect has been previously observed in Ru-1222 at $T = 16$ K, which is about 30 K below T_{SC}, in samples made using an oxygen flow [41].

The temperature dependence of H_{c1} can be understood when the magnetism of the Ru sublattice is properly considered. A model for the magnetic properties of the Ru-1212 system that incorporates the theory of the superconducting/ferromagnetic multilayers predicts an increase in H_{c1} with the decrease in temperature [42]. This response was obtained assuming $T_M \gg T_{SC}$, which is the case for both Ru-1222 and Ru-1212 compounds, and ascribed to the decrease of the effective Josephson coupling between the SC planes due to the exchange field at the FM layers. In addition, the mentioned $1/\lambda^2(T)$ dependence for Ru-1222 supports the increase of H_{c1} as the temperature diminishes, within the framework of a BCS-type behavior. Under this assumption, the strong increase in $1/\lambda^2(T)$ with the rise of the oxygen pressure supports a significant increase of H_{c1} for the *hop* sample.

The order of magnitude of J_c was determined using the expression $J_c = H^*/(d/2)$, corresponding to the Bean critical state model for an infinite SC slab [23], with $d \cong 1$ μm and $H^* = (H_{sat} - H_{c1})/2$. The expression for an infinite slab gives the highest possible values for J_c according to the geometry of the SC grain. For a cylindrical geometry there will be a decrease by one order of magnitude. Therefore, the calculated values $J_c \sim 10^7$ A/cm^2 should be considered as an upper limit. This large order of magnitude can be explained in terms of the magnetic phase separation scenario [27]. Ferromagnetic nanoclusters in the normal state are embedded in an antiferromagnetic matrix in which superconductivity nucleates. Since the SC coherence length ξ for Ru-1222 is about the same size as the magnetic clusters [12], they can effectively act as pinning centers. The monotonic increase of J_c with the decrease in temperature can also be qualitatively explained in terms of the segregation of FM clusters. It has been demonstrated for Ru-1222(Eu) that the saturation magnetization of this magnetic species monotonically increases on cooling down to 10 K [27], well inside the SC region. This result is due to an increase of the density of FM clusters and/or to variation of their sizes with the decrease in temperature. As the number of magnetic clusters increases at lower temperatures, the average matching between the Abrikosov lattice and the spatial arrangement of pinning-cluster centers is gradually improved.

Finally, it is worth noticing that while oxygenation under pressure increases the values of H_{c1} by nearly a factor of two at low temperatures, the increase in J_c is moderate. These results suggest that the oxygen treatment has a larger effect in the region near the grain boundaries. Flux penetration begins at lower fields for the *asp* sample because a larger deviation from the oxygen stoichiometry at the grain borders locally depresses superconductivity. Since J_c is influenced by the properties of the grain as a whole it is less affected by the oxygenation process. The significant decrease of the absolute resistivity values and

the reduction in the width of the SC transition for the *hop* sample in comparison to the *asp* one, while the intragrain SC transition temperature increases only by ∼3 K, confirm that the intergranular connectivity is greatly improved with oxygenation under pressure, while the core of the grains change in a much less extent.

5 Conclusions

In summary, fundamental characteristic properties of Ru-1222, the lower critical field of the grains and the intragrain critical current density, were determined after a detailed processing of magnetoresistance loops, $R(H)$. The H_{c1} values at low temperatures in well oxygenated samples are about fifty times larger than the naive estimation obtained from magnetization measurements at low magnetic fields; the magnitude of J_c is similar to the high-T_c cuprates. The possible segregation of normal-state ferromagnetic nanoclusters provides a natural scenario to explain the monotonic increase of both $H_{c1}(T)$ and $J_c(T)$ on cooling.

We thank S. Smansunaga and R. Jardim for assistance with sample oxygenation under high pressures, and E. Altshuler for useful comments. This work was partially financed by CNPq and Faperj. S.G. was supported by CAPES.

References

1. L. Bauernfeind, W. Widder, H.F. Braun, Physica C **254**, 151 (1995)
2. J.L. Tallon, C. Bernhard, M.E. Bowden, P.W. Gilberd, T.M. Stoto, Pringle, IEEE Trans. Appl. Supercond. **9**, 1696 (1999)
3. For a recent review see T. Nachtrab, C. Bernhard, C.T. Lin, D. Koelle, R. Kleiner, to be published in Journal Comptes Rendus de l'Academie des Sciences (Comptes Rendus Physique), Special Issue on "Magnetism and Superconductivity Coexistence", e-print `arXiv:cond-mat/0508044` (unpublished)
4. W.E. Pickett, R. Weht, A.B. Shick, Phys. Rev. Lett. **83**, 3713 (1999)
5. Ada López, I. Souza Azevedo, J.E. Musa, E. Baggio-Saitovitch, S. Garcia Garcia, Phys. Rev. B **68**, 134516 (2003)
6. T. Nachtrab, D. Koelle, R. Kleiner, C. Bernhard, C.T. Lin, Phys. Rev. Lett. **92**, 117001 (2004)
7. J.E. McCrone, J.R. Cooper, J.L. Tallon, J. Low Temp. Phys. **117**, 1199 (1999)
8. J.L. Tallon, J.W. Loram, G.V.M. Williams, C. Bernhard, Phys. Rev. B **61**, R6471 (2000)
9. J.E. McCrone, J.L. Tallon, J.R. Cooper, A.C. MacLaughlin, J.P. Attfield, C. Bernhard, Phys. Rev. B **68**, 064514 (2003)
10. Y.Y. Xue, D.H. Cao, B. Lorenz, C.W. Chu, Phys. Rev. B **65**, 020511(R) (2001)
11. Y.Y. Xue, B. Lorenz, A. Baikalov, D.H. Cao, Z.G. Li, C.W. Chu, Phys. Rev. B **66**, 014503 (2002)
12. M.T. Escote, V.A. Meza, R.F. Jardim, L. Ben-Dor, M.S. Torikachvili, A.H. Lacerda, Phys. Rev. B **66**, 144503 (2002)
13. M.R. Cimberle, M. Tropeano, M. Ferretti, A. Martinelli, C. Artini, G.A. Costa, Supercond. Sci. Technol. **18**, 454 (2005)
14. C. Attanasio, M. Salvato, R. Ciancio, M. Gombos, S. Pace, S. Uthayakumar, A. Vecchione, Physica C **411**, 126 (2004)
15. Y.Y. Xue, B. Lorenz, R.L. Meng, A. Baikalov, C.W. Chu, Physica C **364–365**, 251 (2001)
16. S. Garcia, L. Ghivelder, Phys. Rev. B **70**, 052503 (2004)
17. B. Lorenz, Y.Y. Xue, R.L. Meng, C.W. Chu, Phys. Rev. B **65**, 174503 (2002)
18. V.P.S. Awana, E. Takayama-Muromachi, M. Karppinen, H. Yamauchi, Physica C **390**, 233 (2003)
19. I. Felner, U. Asaf, Y. Levi, O. Millo, Phys. Rev. B **55**, R3374 (1997)
20. I. Felner, U. Asaf, S.D. Goren, C. Korn, Phys. Rev. B **57**, 550 (1998)
21. I. Felner, E. Galstyan, Int. J. Mod. Phys. B **17**, 3617 (2003)
22. S. Garcia, J.E. Musa, R.S. Freitas, L. Ghivelder, Phys. Rev. B **68**, 144512 (2003)
23. C.P. Bean, Rev. Mod. Phys. **36**, 31 (1964)
24. I. Felner, E. Galstyan, B. Lorenz, D. Cao, Y.S. Wang, Y.Y. Xue, C.W. Chu, Phys. Rev. B **67**, 134506 (2003)
25. C.A. Cardoso, F.M. Araujo-Moreira, V.P.S. Awana, E. Takayama-Muromachi, O.F. de Lima, H. Yamauchi, M. Karppinen, Phys. Rev. B **67**, 020407(R) (2003)
26. E.B. Sonin, I. Felner, Phys. Rev. B **57**, R14 000 (1998)
27. Y.Y. Xue, B. Lorenz, D.H. Cao, C.W. Chu, Phys. Rev. B **67**, 184507 (2003)
28. H.K. Lee, G.V.M. Williams, Physica C **415**, 172 (2004)
29. C.S. Knee, B.D. Rainford, M.T. Weller, J. Mater. Chem. **10**, 2445 (2000)
30. I. Zivkovic, Y. Hirai, B.H. Frazer, M. Prester, D. Drobac, D. Ariosa, H. Berger, D. Pavuna, G. Margaritondo, I. Felner, M. Onellion, Phys. Rev. B **65**, 144420 (2002)
31. M.G. das Virgens, S. Garcia, M.A. Continentino, L. Ghivelder, Phys. Rev. B **71**, 064520 (2005)
32. E. Altshuler, S. Garcia, J. Barroso, Physica C **177**, 61 (1991)
33. D.H. Wu, S. Sridhar, Phys. Rev. Lett. **65**, 2074 (1990)
34. A.C. McLaughlin, W. Zhou, J.P. Attfield, A.N. Fitch, J.L. Tallon, Phys. Rev. B **60**, 7512 (1999)
35. M. Konczykowski, L.I. Burlachkov, Y. Yeshurun, F. Holtzberg, Phys. Rev. B **43**, R13707 (1991)
36. A.E. Koshelev, V.M. Vinokur, Phys. Rev. B **64**, 134518 (2001)
37. G.V.M. Williams, Ho Keun Lee, S. Krämer, Phys. Rev. B **67**, 104514 (2003)
38. I. Felner, E.B. Sonin, T. Machi, N. Koshizuka, Physica C **341–348**, 715 (2000)
39. A. Fainstein, E. Winkler, A. Butera, J. Tallon, Phys. Rev. B **60**, R12 597 (1999)
40. C. Bernhard, J.L. Tallon, Ch. Niedermayer, Th. Blasius, A. Golnik, E. Brücher, R.K. Kremer, D.R. Noakes, C.E. Stronach, E.J. Ansaldo, Phys. Rev. B **59**, 14 099 (1999)
41. C. Bernhard, J.L. Tallon, E. Brücher, R.K. Kremer, Phys. Rev. B **61**, R14 960 (2000)
42. M. Houzet, A. Buzdin, M.L. Kulić, Phys. Rev. B **64**, 184501 (2001)